

# The Characterization of Silicon Wettability and Properties of Externally Wetted Microfabricated Electro spray Thruster Arrays

IEPC-2005-195

Presented at the 29<sup>th</sup> International Electric Propulsion Conference, Princeton University,  
October 31 – November 4, 2005

Tanya Cruz Garza<sup>\*</sup>, Paulo Lozano<sup>†</sup>, Luis F. Velásquez-García<sup>‡</sup>, and Manuel Martinez Sanchez<sup>§</sup>  
Massachusetts Institute of Technology, Cambridge, MA, 02139, USA

**Abstract:** This research explores the parameters that affect wettability of externally wetted microfabricated silicon electro spray thruster arrays and how varied wetting surface treatments affect thruster performance. Silicon wettability is analyzed by producing samples with various black silicon treatments and then measuring contact angle, measuring surface roughness, imaging surface geometry, calculating spreading rates, and performing treated thruster current output tests. Two propellants, 1-ethyl-3-methyl-imidazolium tetrafluoroborate (EMI-BF<sub>4</sub>) and 1-ethyl-3-methyl-imidazolium bis(trifluoromethyl-sulfonyl)amide (EMI-IM), were used in contact angle measurements. Spreading rates and thruster performance of EMI-BF<sub>4</sub> were measured. The forces dominating spreading are extracted from the data. Results from these measurements and experiments indicate that a 9 minute Cl/He plasma treatment with high bias power and pressure produces favorable wetting and optimum thruster performance.

## Nomenclature

$A$	=	drop area
$A_0$	=	initial drop area
$A_{iner}$	=	drop area resulting from inertial forces
$A_{visc}$	=	drop area resulting from viscous forces
$\eta$	=	fluid dynamic viscosity
$K_1$	=	logarithm of a macroscopic droplet size to liquid layer slippage over solid $\cong 10$
$\rho$	=	fluid density
$R$	=	drop base radius
$R_0$	=	initial drop base radius
$s_{LV}$	=	liquid surface tension
$q$	=	drop contact angle
$t$	=	time
$U$	=	triple line velocity
$v$	=	drop volume

---

<sup>\*</sup> Graduate Student, Department of Aeronautics and Astronautics, tanyacg@mit.edu.

<sup>†</sup> Research Scientist, Department of Aeronautics and Astronautics, plozano@mit.edu.

<sup>‡</sup> Research Scientist, Department of Aeronautics and Astronautics/Microsystems Technologies Laboratories, lfvelasq@mit.edu.

<sup>§</sup> Professor, Department of Aeronautics and Astronautics, mmart@mit.edu.

## I. Introduction

WHEN the meniscus of a conducting liquid is immersed in a sufficiently strong electric field, the liquid forms a conical structure known as a Taylor cone caused by the balance between electrostatic traction and the surface tension forces in the liquid.<sup>1</sup> This configuration can produce a structure known as a cone jet in which a thin jet of charged particles and droplets are emitted from the cone tip. The liquid can either be supplied from a capillary or from an externally wetted surface to make an electrospray thruster.

Arrays of externally wetted electrospray thrusters can be batch fabricated using microfabrication techniques on silicon allowing the amount of thrust provided to be increased. An untreated silicon surface is not particularly wettable by fluids including the ionic liquids 1-ethyl-3-methyl-imidazolium tetrafluoroborate (EMI-BF<sub>4</sub>) and 1-ethyl-3-methyl-imidazolium bis(trifluoromethylsulfonyl)amide (EMI-IM), which have been shown to work as electrospray propellants.<sup>2,3</sup> It has been shown that the wettability of silicon can be improved by treating the surface and forming black silicon.<sup>4</sup> Black silicon or porous silicon is produced by plasma etching silicon to make the surface rough, thus facilitating the propellant transport over the thruster surfaces and promoting current output. It is desirable to understand how black silicon treatments can be optimized to produce wettable thrusters with favorable performance. This paper explores the parameters that affect wettability of externally wetted silicon electrospray thruster arrays.

## II. Methods

Silicon wettability was analyzed by producing samples with various black silicon treatments and performing five analyses: atomic force microscope (AFM) measurements to determine average surface roughness, contact angle measurements with the EMI-BF<sub>4</sub> and EMI-IM, scanning electron microscope (SEM) measurements to determine surface geometry, spreading rate experiments to analyze dynamic wetting properties, and thruster tests to verify thruster current output.

### A. Wettability Treatments and Fabrication

Black silicon treatments were done with a PlasmaQuest Electron Cyclotron Resonance (ECR) plasma etcher. Treatments were done with varied Cl/He working gas flow rates, bias power levels, source power levels, chamber pressures, and etch times. Table 1 shows all the samples fabricated and values of etch parameters. Treatments were numbered 1, 2, 3, 4, 1', 2', 3', 4', 5', 6', 7', 8', 9', 10', 11', 12', 1'', 2'', 3'', and 4''.

**Table 1. Etch parameters for silicon samples made to test wettability.**

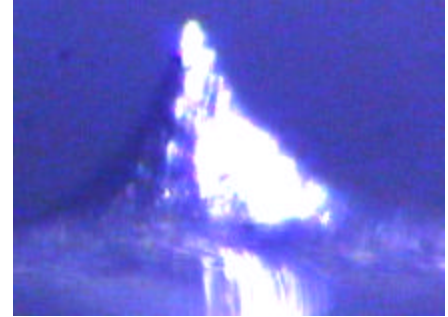
Etch Times	Low Values	High He	High Press	High Bias	High Power
5 min	1			4	2
5 min				3	
7.5 min	1'		5'	4'	2'
7.5 min				3'	
9 min		9'	8'	7'	
9 min			10'		
9 min		12'			
9 min		11'			
10 min		3''	2''	1''	
10 min			4''		

Key of Parameters		
6' - plain silicon		
Chlorine flowrate for all samples: 120 sccm		
	High Value	Low Value
Helium Flow -	60 sccm	30 sccm
Pressure -	25 mTorr	50 mTorr
Bias Power -	20 W	40 W
Source Power -	200 W	400 W

Note: Shaded boxes contain sample #'s  
 Note: Unless otherwise indicated, all parameters for a given sample are at the low value.

The thrusters to which the black silicon treatment was applied and which were used for testing were pointed pyramidal emitters. A single emitter is pictured in Fig. 1. These thrusters were a variation in design of the pencils described in Ref. 4. The difference between these thrusters and the pencil design is that they lack an anisotropic etch which gives it the final pencil shape and they have the varied final black silicon treatments described in Table 1. Each tested array had a 8 mm x 8 mm active area and contained 16 emitters (4 x 4).<sup>5</sup>



**Figure 1. Single emitter.**  
Close up of single emitter of 4x4 externally wetted silicon emitter array.

### B. Experimental Setup and Hardware

Both AFM and SEM were used to produce images of the black silicon surfaces and determine average surface roughness. An Autoprobe CP Atomic Force Microscope was used for AFM measurements. A Ramé-hart contact angle goniometer model 100 was used to find static contact angle measurements. The contact angle of three to six drops of sizes ranging from a few hundred nL to a few  $\mu\text{L}$  of each propellant per sample was measured no more than a minute after the drop was placed on the sample surface. The contact angles measured were not always at their equilibrium value. The near-zero contact angles are less accurate than the large contact angles measured because these samples did not reach an equilibrium value within a minute and continued to spread.

Spreading rate experiments consisted of video taping the spread of a 1  $\mu\text{L}$  sessile drop on a sample and using Matlab to analyze its increase in area with time. From the known size of the roughened silicon sample an approximate initial area of the drop could be determined. The camera pictures were taken at a  $\sim 45^\circ$  angle to the samples and the images were assumed two dimensional in the area analysis, introducing a source of error. The repeatability of the experiment and comparability of the results was also limited by the lack of control of the initial area of the drop on the silicon surface.

The experimental setup for the thruster array tests consisted of 4 parts diagramed in Fig. 2. The first was the 4 x 4 silicon emitter array (a). A stainless steel extractor (b) with 1.8 mm diameter holes was suspended approximately 1.4 mm in front of the emitters. A negative potential of 3 kV was applied between the emitter and the grounded extractor. A tungsten grid (c) was suspended in front of the emitter/extractor assembly and biased to -50 V to suppress secondary electron emission. The final portion of the experimental setup consisted of a stainless steel collector plate (d). A Keithley 6514 electrometer was used to measure the current collected by the collector plate. The entire experimental assembly was kept at room temperature inside a vacuum chamber with a pressure less than  $2 \times 10^{-6}$  Torr.

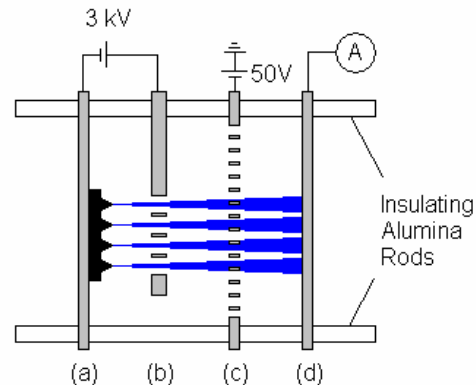


**Figure 2. Experimental setup for thruster tests.**  
Diagram of experimental setup used to test 4x4 silicon thruster arrays with black silicon treatment.

### III. Results

The results are arranged in an order corresponding to the elimination process for optimal sample selection. Each measurement or experiment provided data that allowed us to disregard treatments that were unlikely candidates for favorable externally wetted thruster performance.

#### A. AFM Measurements

The average surface roughness values of the surfaces are plotted in Fig. 3. According to Table

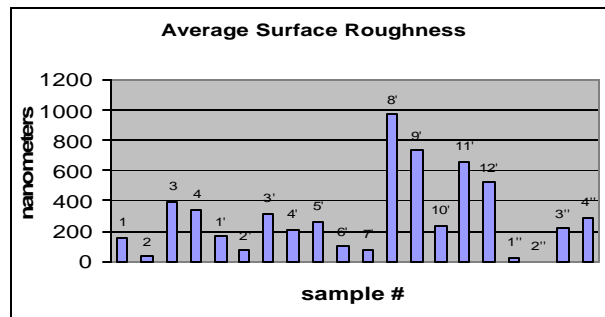
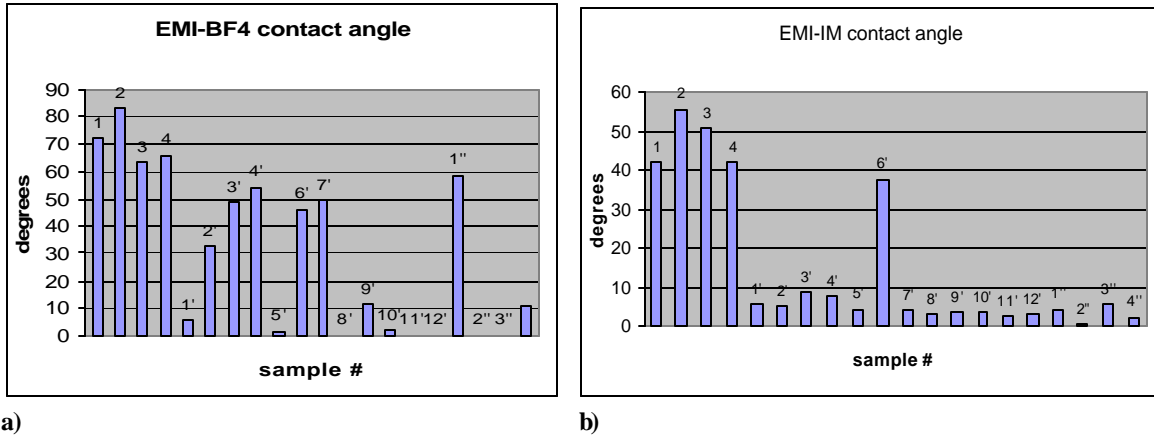


**Figure 3. Plot of average sample surface roughness.**  
Average of the magnitude of surface height deviations from the average surface height found from AFM measurements.

1, rougher samples were produced by the 9 minute treatments as opposed to longer treatments. This trend implies that the treatment roughness reaches a maximum with respect to etch time. The general assumption is that the rougher the sample surface is the greater wettability it will have (assuming roughness peaks are not too large). Thus, the rougher surfaces were considered better candidates for wettability.

### B. Contact Angle Measurements

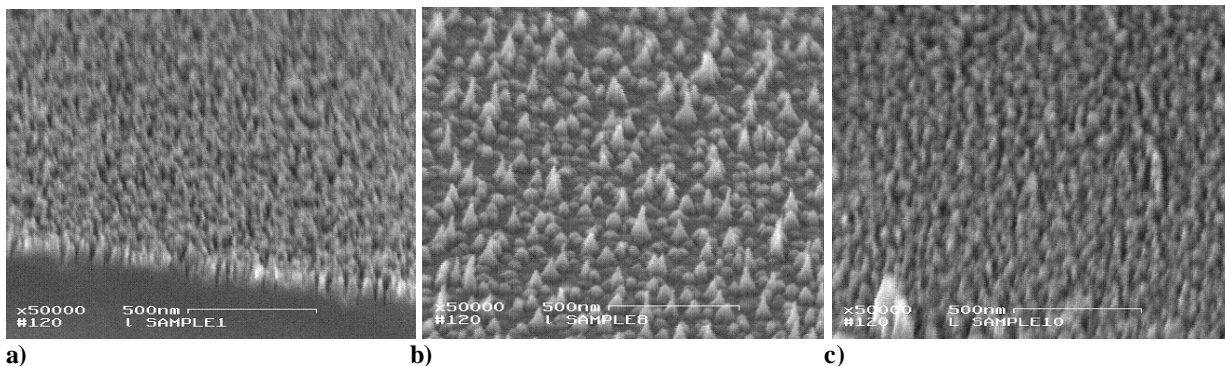
Contact angle measurements of both EMI-BF<sub>4</sub> and EMI-IM on the samples were made. These measurements are displayed in Fig. 4. By definition, a surface is considered wettable if it has a contact angle less than 90°. Thus, the lower a contact angle a surface has, the more wettable it is. It is somewhat counterintuitive that samples 1', 5', 10', 2'', and 3'' with small roughness values seen in Fig. 3 had fairly low measured contact angles seen in Fig. 4.



a) **Figure 4. Plot of average contact angle.**  
Average contact angle measurements of a) EMI-BF<sub>4</sub> and b) EMI-IM on silicon samples with various black silicon

### C. SEM Measurements

Eight of the samples were selected to test spreading rate and take SEM measurements. These were samples 2, 2'', 5', 8', 9', 10', 11', and 12'. Sample 2 had one of the lowest roughness and the highest contact angle and thus was picked for comparison purposes. The remaining samples were chosen because they had lower contact angles and thus were considered “good” samples. Figure 5 shows the surfaces of samples 2, 8', and 10', all at the same magnification.



a) **Figure 5. SEM images of selected black silicon surfaces.**  
SEM images taken at a 30° angle with 500 nm resolution of samples a) 2, b) 8' and c) 10'

It is interesting to note that, although sample 2 had the lowest measured roughness, its surface does not appear smooth. Figure 5 shows that sample 2 actually has close packed peaks. The closeness of the large peaks in sample 2 may have been outside the AFM depth resolution thus causing the surface to appear smooth. A close look at sample 8' shows tall peaks with smooth gaps between them. These tall peaks would explain why sample 8' had the largest value of average surface roughness. The smooth spaces between the large peaks of sample 8' might suggest that its

surface could have wetting problems and perhaps slow spreading rates. Sample 10' had a fairly average surface roughness but Fig. 5 shows peaks which are closely spaced.

Figure 6 shows samples 2", 5', and 9' which had smoother surfaces than those samples shown in Fig. 5 yet, these samples have small contact angles, an effect not currently understood.

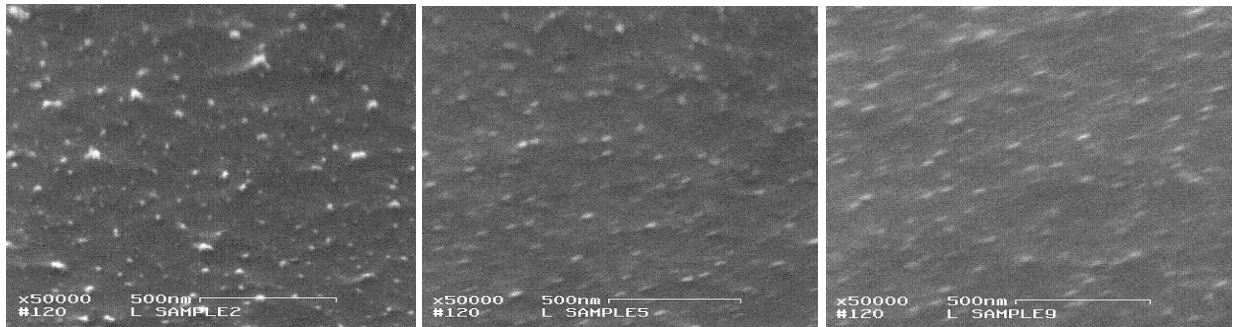


**Figure 6. SEM images of selected black silicon surfaces.**  
SEM images taken at a 30° angle with 500 nm resolution of samples a) 2α b) 5ζ and c) 9ζ

#### D. Spreading Rate Experiments

Spreading rate measurements results are plotted in Fig. 7. Although sample 8' had the largest roughness value, it had fairly average spreading. This contradiction could possibly be explained by the smooth spaces between the large peaks noted in the SEM images. It is also interesting to note that sample 2" was the least rough sample and yet had an average spreading rate. Figure 7 shows that sample 10' had the largest spreading rate.

Sessile drop spreading is influenced by inertial and viscous forces in the absence of other external forces.<sup>6</sup> Inertial spreading is expected to take place over a short period of time while the drop quickly settles on the surface. Viscous spreading is then expected to control the bulk of drop spreading. We will analyze this hypothesis here.

For inertial spreading, assume the drop takes a circular base area  $A$  with an initial radius  $R_0$ . According to Ref. 6, a balance of capillary energy and kinetic energy implies:

$$U \cong \left[ \frac{\sigma_{LV}}{\rho R_0} \right]^{1/2}, \quad (1)$$

where  $U$  is the liquid, solid, vapor triple line velocity (such that  $U = dR/dt$ , the rate of change of the drop radius  $R$  with respect to time  $t$ ),  $\sigma_{LV}$  is the liquid surface tension, and  $\rho$  is the liquid density. Since  $\sigma_{LV}$ ,  $\rho$ , and  $R_0$  are

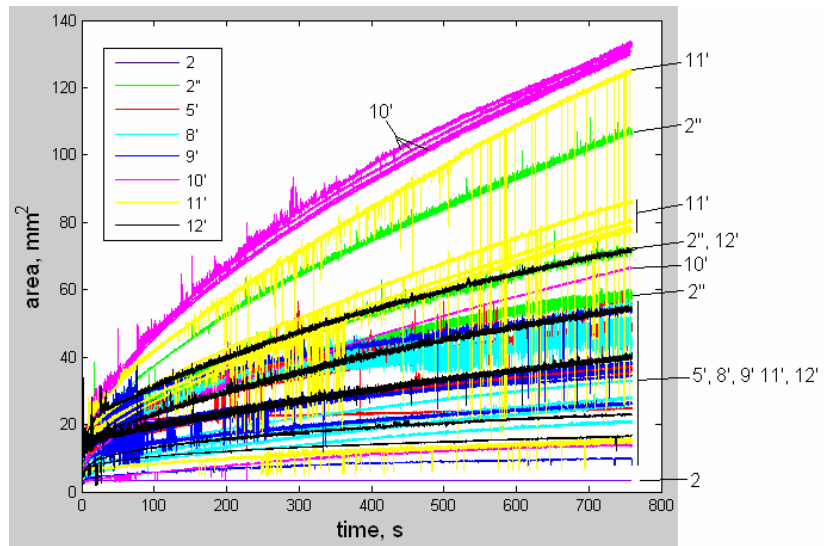


**Figure 7. Spreading rate data.**  
Plots of drop areas versus time for an  $nL$  drop on various black silicon samples. Samples 10ζ 11ζ and 2α are the topmost plots indicating largest spreading.

constants for the given conditions,  $U$  is a constant value. The increase of drop area is governed by the following equation

$$A = \mathbf{p}[R_0 + Ut]^2, \quad (2)$$

The substitution of (1) into (2) yields the following equation for area versus time

$$A_{iner} = \mathbf{p} \left[ R_0 + \left( \frac{\mathbf{s}_{LV}}{rR_0} \right)^{1/2} t \right]^2, \quad (3)$$

where  $A_{iner}$  indicates area that is predicted by inertial forces.

For viscous spreading, an argument given by Ref. 6 balances viscous energy dissipation with change in surface and interfacial energy to reach a relation between triple line velocity and contact angle  $\theta$ . Making small angle approximations and assuming a circular drop base area, the following relation is obtained:

$$R^{10} - R_0^{10} = A_1 t, \quad (4)$$

where  $A_1 \cong 3\sigma_{LV}^3/(\eta K_1)$  with  $v$  as the volume of the drop,  $\eta$  is the dynamic viscosity, and  $K_1$  is the logarithm of a macroscopic droplet size to liquid layer slippage over the solid  $\cong 10$ .

$$A_{visc} = \mathbf{p} [R_0^{10} + A_1 t]^{1/5} \quad (5)$$

Equations (3) and (5) can be differentiated with respect to time to give the following:

$$\frac{dA_{iner}}{dt} = 2\mathbf{p} \left[ R_0 + \left( \frac{\mathbf{s}_{LV}}{rR_0} \right)^{1/2} t \right] \left( \frac{\mathbf{s}_{LV}}{rR_0} \right)^{1/2} \quad (6)$$

and

$$\frac{dA_{visc}}{dt} = \frac{\mathbf{p}A_1}{5} [R_0^{10} + A_1 t]^{-4/5} \quad (7)$$

Consider EMI-BF<sub>4</sub> with values of  $\sigma_{LV} = 0.052$  N/m,  $\rho = 1294$  kg/m<sup>3</sup>,  $\eta = 3.56 \times 10^{-3}$  kg/(ms), a volume  $v = 1$   $\mu$ L,  $R_0 = 10^{-3}$  m, and  $t = 10$  s. This data gives values of  $dA_{iner}/dt = 5.33 \times 10^{-7}$  m<sup>2</sup>/s and  $dA_{visc}/dt = 2.51$  m<sup>2</sup>/s suggesting that the inertial forces are quickly over powered by the viscous effects.

This result suggests that a linear fit could be made with the area to the fifth power versus time data shown in Fig. 7. On a log scale this results in slopes ranging  $-0.15$  to  $0.25$ , or an average of  $0.2$ . This behavior fits the viscous spreading model.

## E. Thruster Current Measurement

Samples  $\mathcal{Z}'$ ,  $10'$ , and  $\mathcal{G}$  were chosen as likely candidates for producing favorable thruster performance. These treatments were applied to  $4 \times 4$  emitter arrays and tested with the conditions outlined in section II.B. Of the three, only sample  $10'$  produced current. (Current is not reported here because the data is preliminary and was intended to measure of thruster function. Setup configuration would need to be adjusted to get an accurate measure of current output.)

## IV. Conclusion

Based on AFM and SEM imaging, contact angle measurements, spreading rate experiments, and thruster current measurements, it has been determined that a black silicon plasma treatment with a 50 mTorr chamber pressure and 40 W bias power operating for 9 minute with a 200 W source power produces a favorable silicon wettability and favorable performance on externally wetted microfabricated silicon electrospray thrusters. Spreading rate experiments suggest that the spread of EMI-BF<sub>4</sub> on a black silicon surface is dominated by viscous forces after a few minutes of initial spreading.

## Acknowledgments

T.C. Garza would like to thank the MIT Microtechnologies Laboratory staff for their experienced assistance, and the students of the MIT Space Propulsion Lab for their support and ideas with a special thanks to Félix Parra-Díaz, Justin Pucci, and Murat Çelik for their intellectual assistance. T. C. Garza would also like to give a special thanks to Liang-Yu Chen for her help with SEM images.

T.C. Garza would like to thank the GEM fellowship program for their financial support as well as the Air Force Office of Scientific Research (AFOSR), Mitat Birkan technical monitor and Darpa, MGA program, Clark Nguyen project manager.

## References

- <sup>1</sup>Taylor, G. I., "Distintegration of Water Drops in an Electric Field," *Proc. R. Soc. London A*, Vol. 280, No. 1382, 1964, pp. 383-397.
- <sup>2</sup>Lozano, P., and Martínez-Sánchez, M., "Ionic Liquid Ion Sources: Characterization of Externally Wetted Emitters," *Journal of Colloid and Surface Science*, Vol. 282, Issue 2, 15 Feb. 2005, pp. 415-421.
- <sup>3</sup>Camero-Castaño, M., and Hruby, V., "Electrospray as a Source of Nanoparticles for Efficient Colloid Thrusters," *Journal of Propulsion and Power*, Vol. 17, No. 5, Sept-Oct 2001.
- <sup>4</sup>Velásquez-García, L. F., Akinwande, A. I., and Martínez-Sánchez, M., "A Planar Array of Micro-fabricated Electrospray Emitters for Thruster Applications," *Journal of Microelectromechanical Systems* (to be published).
- <sup>5</sup>Velásquez-García, "The Design, Fabrication and Testing of Micro-fabricated Linear and Planar Colloid Thruster Arrays," Ph.D. Dissertation, Aeronautics and Astronautics Dept., Massachusetts Institute of Technology, Cambridge, MA, 2004.
- <sup>6</sup>Eustathopoulos, N., Nicholas, M. G., and Drevet, B., *Wettability at High Temperatures*, Vol. 3, Pergamon Materials Series, Oxford, England, UK, 1999, Chap. 2.